Localization of Autocrine Motility Factor Receptor to Caveolae and Clathrin-independent Internalization of Its Ligand to Smooth Endoplasmic Reticulum

Naciba Benlimame, Phuong U. Le, and Ivan R. Nabi*

Département de Pathologie et Biologie Cellulaire, Université de Montréal, Montréal, Québec, Canada H3C 3J7

Autocrine motility factor receptor (AMF-R) is a cell surface receptor that is also localized to a smooth subdomain of the endoplasmic reticulum, the AMF-R tubule. By postembedding immunoelectron microscopy, AMF-R concentrates within smooth plasmalemmal vesicles or caveolae in both NIH-3T3 fibroblasts and HeLa cells. By confocal microscopy, cell surface AMF-R labeled by the addition of anti-AMF-R antibody to viable cells at 4°C exhibits partial colocalization with caveolin, confirming the localization of cell surface AMF-R to caveolae. Labeling of cell surface AMF-R by either anti-AMF-R antibody or biotinylated AMF (bAMF) exhibits extensive colocalization and after a pulse of 1–2 h at 37°C, bAMF accumulates in densely labeled perinuclear structures as well as fainter tubular structures that colocalize with AMF-R tubules. After a subsequent 2- to 4-h chase, bAMF is localized predominantly to AMF-R tubules. Cytoplasmic acidification, blocking clathrin-mediated endocytosis, results in the essentially exclusive distribution of internalized bAMF to AMF-R tubules. By confocal microscopy, the tubular structures labeled by internalized bAMF show complete colocalization with AMF-R tubules. bAMF internalized in the presence of a 10-fold excess of unlabeled AMF labels perinuclear punctate structures, which are therefore the product of fluid phase endocytosis, but does not label AMF-R tubules, demonstrating that bAMF targeting to AMF-R tubules occurs via a receptor-mediated pathway. By electron microscopy, bAMF internalized for 10 min is located to cell surface caveolae and after 30 min is present within smooth and rough endoplasmic reticulum tubules. AMF-R is therefore internalized via a receptor-mediated clathrin-independent pathway to smooth ER. The steady state localization of AMF-R to caveolae implicates these cell surface invaginations in AMF-R endocytosis.

INTRODUCTION

Expression of autocrine motility factor receptor (AMF-R) is associated with the acquisition of motile and metastatic properties by tumor cells (for review see Silletti and Raz, 1996). AMF-R expression correlates with the malignancy of human bladder, colon, and gastric tumors (Nakamori *et al.*, 1994; Otto *et al.*, 1994; Hirono *et al.*, 1996). In cultured cells, AMF-R expression is decreased in contact-inhibited A31–3T3 fibroblasts (Silletti and Raz,

1993) and increased after viral transformation of MDCK epithelial cells (Simard and Nabi, 1996). AMF-R is a cell surface receptor that mediates motility stimulation by its 55-kDa polypeptide ligand, AMF, recently shown to be homologous to phosphohexose isomerase (Liotta *et al.*, 1986; Watanabe *et al.*, 1996). AMF is selectively secreted after transformation of NIH-3T3 cells, and the presence of AMF activity in the urine of cancer patients correlates with tumor malignancy (Liotta *et al.*, 1986; Guirguis *et al.*, 1990).

Transduction of the AMF motility signal occurs via receptor phosphorylation, a pertussis toxin-sensitive

* Corresponding author.

G-protein, inositol phosphate production, tyrosine kinase and PKC activation, and production of the lipoxygenase metabolite 12-HETE (Silletti and Raz, 1996). AMF-R is localized not only to the plasma membrane but also to an intracellular tubular organelle, the AMF-R tubule (Nabi *et al.*, 1992; Benlimame *et al.*, 1995). AMF-R tubules are distinct from endosomes and lysosomes; by postembedding immunoelectron microscopy AMF-R is present primarily in smooth tubules that extend from ribosome-studded cisternae; however, AMF-R tubules do not colocalize with ER-GIC-53, a marker for the ER–Golgi intermediate compartment (Benlimame *et al.*, 1995; Wang *et al.*, 1997). After treatment with ilimaquinone, which induces vesiculation of the Golgi apparatus (Takizawa *et al.*, 1993), AMF-R tubules acquire a fenestrated morphology typical of smooth ER, suggesting that the AMF-R tubule is a distinct smooth subdomain of the ER (Wang *et al.*, 1997). The intracellular distribution of this cell surface receptor to smooth ER implicates AMF-R recycling in its function in cell motility and tumor cell metastasis.

Actin cytoskeleton reorganization at the leading edge and de novo establishment of cell–substrate contacts results in lamellipodial extension and the consequent polarization of the motile cell (Rinnerthaler *et al.*, 1988; Condeelis, 1993; Stossel, 1993). The role of intracellular vesicular traffic in the establishment and maintenance of epithelial and neuronal polarity is well-established (Rodriguez-Boulan and Powell, 1992; Drubin and Nelson, 1996; Keller and Simons, 1997) and strongly supports a role for intracellular membrane traffic in the polarization of the motile cell and formation of a distinct plasma membrane domain, the leading lamella (Singer and Kupfer, 1986; Nabi *et al.*, 1992; Bretscher, 1996). Influenza hemagglutinin and vesicular stomatitis virus G proteins, polarized apically and basolaterally in epithelial cells and axonally and dendritically in neurons (Rodriguez-Boulan and Sabatini, 1978; Dotti and Simons, 1990), also follow distinct pathways to the cell surface in "unpolarized" fibroblasts (Yoshimoro *et al.*, 1996). Newly synthesized VSV G protein is targeted to the leading edge and cellular protrusions of motile fibroblasts, and the directionality of its delivery was shown to be microtubule-dependent (Bergmann *et al.*, 1983; Rogalski *et al.*, 1984; Peränen *et al.*, 1996). Membrane recycling via coated pits has long been suggested to be implicated in cell spreading and cell motility (Bretscher, 1984). We show here that AMF-R is concentrated at the cell surface within smooth plasmalemmal vesicles or caveolae and that AMF is internalized via a nonclathrin pathway to intracellular smooth ER tubules. Our results implicate caveolae in transduction of the AMF motility signal as well as in the internalization of its receptor.

MATERIALS AND METHODS

Cells and Cell Culture

NIH-3T3 fibroblasts obtained from the ATCC were cloned, and a highly spread clone was used for these studies. HeLa and NIH-3T3 cells were grown in an air-5% CO_2 incubator at constant humidity in DMEM containing nonessential amino acids, vitamins, glutamine, and a penicillin–streptomycin antibiotic mixture (Life Technologies, Burlington, Ontario, Canada) supplemented with 5% FCS (Immunocorp, Montreal, Quebec, Canada) for HeLa or 10% calf serum (Life Technologies) for NIH-3T3 cells.

Antibodies and Chemicals

Monoclonal antibody against AMF-R was used in the form of concentrated hybridoma supernatant (Nabi *et al.*, 1990). Rabbit anti-caveolin polyclonal antibody was purchased from Transduction Laboratories (Lexington, KY), rabbit anti-biotin antibody was purchased from Sigma (St. Louis, MO), and rat anti-LAMP-1 was purchased from the Developmental Studies Hybridoma Bank (University of Iowa, Iowa City, IA). Secondary antibodies conjugated to either fluorescein, Texas Red, or 12-nm gold particles and streptavidin conjugated to fluorescein or Texas Red were purchased from Jackson Immunoresearch Laboratories (West Grove, PA). Texas Red-conjugated human diferric transferrin was kindly provided by Dr. Tim McGraw (Columbia University, New York, NY). Streptavidin conjugated to 10-nm gold particles was purchased from Sigma. The secondary antibodies were designed for use in multiple labeling studies, and no interspecies cross-reactivity was detected. To detect antibodies to AMF-R, secondary antibodies specific for the μ chain of rat immunoglobulin M (IgM) were used.

Rabbit phosphohexose isomerase was purchased from Sigma and biotinylated with NHS-LC-biotin (Pierce, Rockford, IL) according to the manufacturer's instructions. To assess its purity, biotinylated phosphohexose isomerase was separated by SDS-PAGE, transferred to nitrocellulose, probed with HRP-conjugated streptavidin (Jackson Immunoresearch Laboratories) and revealed by chemiluminescence.

Immunofluorescence

Cells were plated on glass cover slips 2 d before each experiment at a concentration of 30,000 cells/35-mm dish. For AMF-R surface labeling, the cells were incubated in DMEM minus bicarbonate supplemented with 25 mM HEPES, pH 7.2, and 2.5% serum for 15 min at 4°C before labeling with anti-AMF-R primary antibody or biotinylated AMF (bAMF) at 4°C for 30 min. The cells were washed at 4°C and then fixed with 3% paraformaldehyde in PBS (pH 7.4) supplemented with 0.1 mM Ca^{++} and 1 mM Mg^{++} (PBS/CM) for 15 min at room temperature. For caveolin labeling, after AMF-R surface labeling at 4°C and fixation as above, the cells were permeabilized with 0.2% Triton X-100 for 10 min, and then extensively washed with PBS/CM containing 1% BSA. The cells were incubated with rabbit anti-caveolin polyclonal antibodies, washed, and then incubated with FITC goat anti-rat IgM to reveal anti-AMF-R and Texas Red donkey anti-rabbit IgG to reveal anti-caveolin. Cell surface labeling with bAMF was revealed with rabbit anti-biotin antibody and fluorescent anti-rabbit secondary antibody.

For the AMF internalization studies, NIH-3T3 cells were pulsed with bAMF (~250–500 μg/ml) and chased at 37°C for the indicated periods of time before fixation by the addition of precooled (−80°C) methanol/acetone directly to the cells. After fixation, internalized bAMF was revealed with Texas Red streptavidin and lysosomes and AMF-R tubules by anti-LAMP-1 and anti-AMF-R antibodies, respectively, followed by the corresponding FITC-conjugated secondary antibodies. Disruption of clathrin-coated pits and vesicles by cytoplasmic acidification was performed essentially as previously described (Heuser, 1989). NIH-3T3 cells were pretreated with acidification medium (DMEM containing 5% calf serum and 50 mM

2-(*N*-morpholino)ethanesulfonic acid, pH 5.5) for 15 min at 37°C before addition of bAMF in acidification medium for 1 h at 37°C. To ensure that cellular acidification blocked clathrin-mediated endocytosis, Texas Red transferrin (50 μg/ml) was added to cells in regular or acidification medium for 30 min at 37°C, after which the cells were fixed with 3% paraformaldehyde.

After labeling, the coverslips were mounted in Airvol (Air Products and Chemicals, Allentown, PA) and viewed in a Zeiss Axioskop fluorescent microscope (Carl Zeiss, Thornwood, NY) equipped with a 63× Plan Apochromat objective and selective filters. Confocal microscopy was performed with the 60× Nikon Plan Apochromat (Nikon, Garden City, NY) objective of a dual channel Bio-Rad MRC600 laser scanning confocal microscope (Bio-Rad, Richmond, CA) equipped with a krypton/argon laser and the corresponding dichroic reflectors to distinguish fluorescein and Texas Red labeling. Confocal images were printed using a Polaroid TX 1500 video printer.

Electron Microscopy

Postembedding immunolabeling for AMF-R was performed as previously described (Benlimame *et al.*, 1995). Cells grown on Petri dishes were rinsed and incubated at 37°C in Ringer's solution for 15 min before being fixed in Ringer's solution containing 2% paraformaldehyde and 0.2% glutaraldehyde for 30 min at 37°C. The fixed cells were rinsed in PBS/CM, scraped from the Petri dish, and collected by centrifugation. The cell pellet was postfixed for 30 min with 1% osmium tetroxide in PBS/CM containing 1.5% potassium ferrocyanide (reduced osmium), dehydrated, and embedded in LR-White resin. Ultrathin sections (80 nm) were blocked with 2% BSA, 0.2% gelatin in PBS/CM for 1 h, and then incubated at room temperature with anti-AMF-R antibody for 1 h followed by 12 nm gold-conjugated goat anti-rat antibodies for 1 h. The sections were then stained with 5% uranyl acetate and examined in a Philips 300 electron microscope. The numerical density of gold particles associated with plasma membrane, caveolae, clathrin-coated pits and vesicles, smooth tubules and vesicles, and rough ER was determined. The length of the limiting membrane of the indicated organelles was measured using a Sigma-Scan measurement system, and the gold particles associated with these organelles were counted. Rough ER was defined by the presence of a linear array of membrane-associated ribosomes. Smooth vesicles attached to the plasma membrane or within 100 nm of the plasma membrane were considered to be caveolae. Control labeling with nonimmune rat IgM antibodies was analyzed similarly.

To follow the endocytic pathway of AMF by electron microscopy, bAMF was internalized as described for the fluorescence studies and detected by postembedding labeling with streptavidin conjugated to 10 nm gold as described above. No labeling was observed in the absence of bAMF.

RESULTS

Localization of AMF-R to Cell Surface Caveolae

By postembedding immunoelectron microscopy in NIH-3T3 and HeLa cells, AMF-R is primarily localized to smooth intracellular membranous tubules (Figure 1, A and D), similar in morphology to those previously described in MDCK cells (Benlimame *et al.*, 1995). At the cell surface, AMF-R label localizes to smooth invaginations of the plasma membrane morphologically equivalent to caveolae (Figure 1, B, C, E, and F). Quantification of the labeling revealed that the predominant AMF-R label is localized to smooth tubules and vesicles, flat regions of the plasma membrane, and caveolae (Table 1). While specific label was previously de-

tected in the rough ER of MDCK cells (Benlimame *et al.*, 1995), the density of labeling of rough ER tubules in NIH-3T3 and HeLa cells is reduced and at control levels. The density of AMF-R labeling of caveolae is equal to that of intracellular smooth tubules and vesicles in NIH-3T3 cells and greater than that of intracellular smooth tubules and vesicles in HeLa cells, and essentially no AMF-R label is found within clathrin-coated pits and vesicles. The density of AMF-R labeling in caveolae is increased relative to flat regions of the plasma membrane. However, based on the total number of gold particles at the plasma membrane, only 13% of cell surface AMF-R in NIH-3T3 and 26% in HeLa cells is found within caveolae.

To assess whether cell surface AMF-R colocalizes with caveolin, viable NIH-3T3 cells were surface labeled for AMF-R by the addition of anti-AMF-R antibodies to the cells at 4°C (Nabi *et al.*, 1992) and then double immunofluorescently labeled after fixation and permeabilization with antibodies to caveolin (Figure 2). While the punctate AMF-R surface label (Figure 2A) did not completely colocalize with the finer caveolin labeling (Figure 2B), confocal microscopy clearly revealed distinct points and patterns labeled for both cell surface AMF-R and caveolin (Figure 2C, yellow). Peripheral regions densely labeled for both AMF-R and caveolin were frequently observed. The partial colocalization of cell surface AMF-R with caveolin is consistent with the fact that, based on the electron microscopic data, only 13% of cell surface AMF-R was localized within the caveolae of NIH-3T3 cells.

Internalization of AMF

The ligand for AMF-R, AMF, is homologous to phosphohexose isomerase (Watanabe *et al.*, 1996). Phosphohexose isomerase (referred to here as AMF) was biotinylated and after separation by SDS-PAGE revealed a single major band after revelation of the blots with streptavidin-HRP (Figure 3A). Cell surface labeling of NIH-3T3 cells by the addition of both bAMF (Figure 3B) and anti-AMF-R at 4°C (Figure 3C) revealed a high degree of colocalization (Figure 3D, yellow), demonstrating that AMF and antibodies to AMF-R recognize the same receptor. The presence of spots labeled exclusively with either bAMF or anti-AMF-R may be due to the fact that the two were added together and may compete for the same site. Indeed, the addition of excess cold AMF before cell surface labeling with anti-AMF-R significantly reduced binding of the antibody (our unpublished observations), as previously demonstrated by immunoblot (Nabi *et al.*, 1990).

Pulse labeling of NIH-3T3 cells with bAMF for 1 or 2 h resulted in the ability to detect both punctate structures as well as fainter tubular structures that colocalized with AMF-R tubules (Figure 4, A and B).
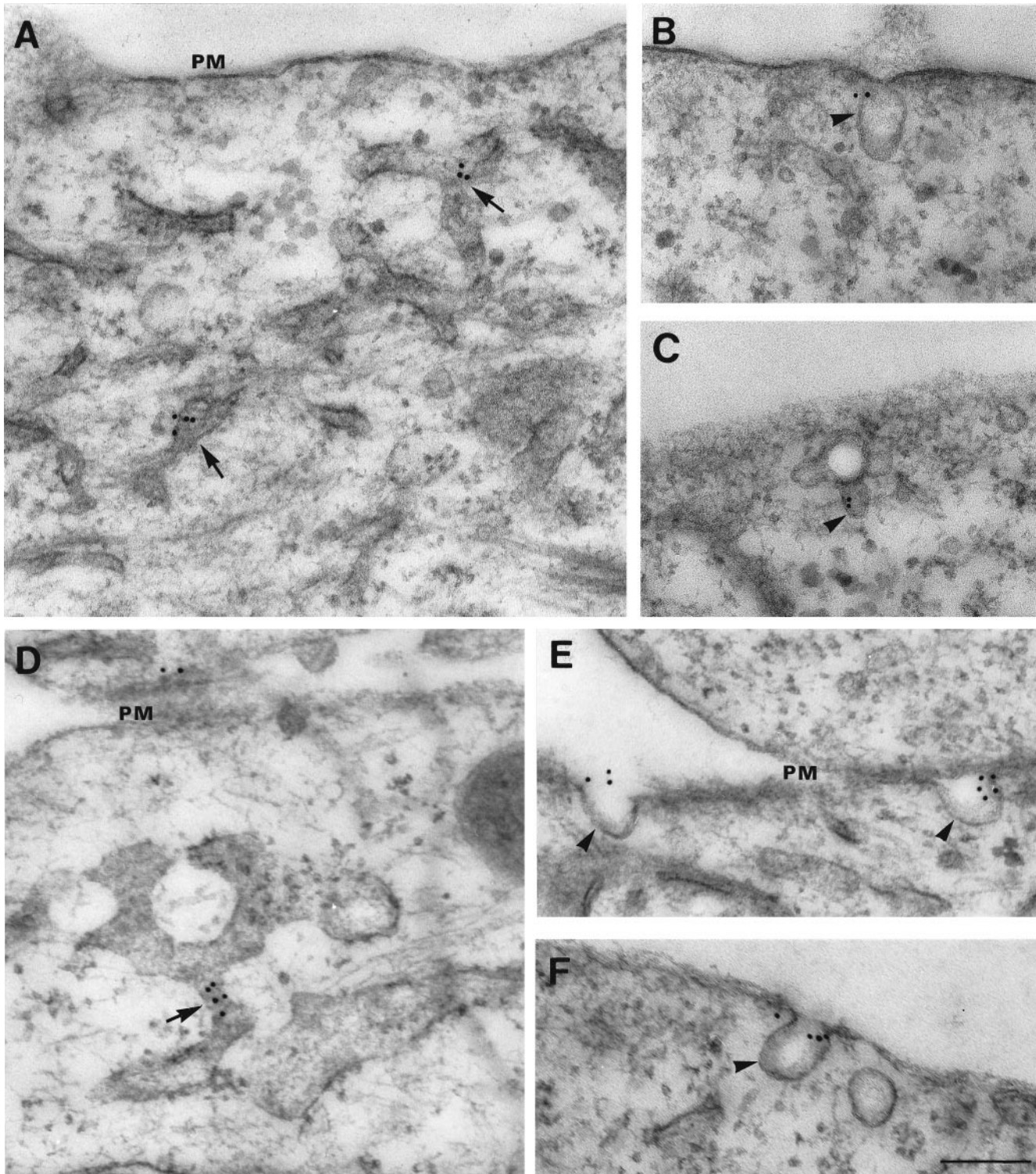
Figure 1. Electron microscopic localization of AMF-R in NIH-3T3 fibroblasts and HeLa cells. HeLa (A, B, and C) and NIH-3T3 (D, E, and F) cells were postembedding immunolabeled with anti-AMF-R and 12-nm gold–conjugated anti-rat IgM secondary antibodies. Typical AMF-R labeling of smooth tubules (A and D, arrows) and cell surface caveolae (B, C, E, F, arrowheads) is shown. PM, Plasma membrane. Bar, 0.2 μm.

Table 1. Localization of AMF-R in HeLa and NIH-3T3 cells by immunoelectron microscopy

	Smooth tubules and vesicles	Rough ER	Flat plasma membrane	Caveolae	Clathrin-coated pits and vesicles
HeLa					
AMF-R					
Gold particles (n)	660	34	147	52	3
Membrane (μm)	328.5	187.5	245.6	14.6	19.3
Gold particles/μm	2.01 ± 0.15	0.18 ± 0.04	0.60 ± 0.08	3.56 ± 0.53	0.16 ± 0.13
Control					
Gold particles (n)	83	6	25	3	1
Membrane (μm)	307.5	95.2	211.0	16.1	5.0
Gold particles/μm	0.27 ± 0.08	0.06 ± 0.03	0.12 ± 0.05	0.19 ± 0.10	0.20 ± 0.21
NIH-3T3					
AMF-R					
Gold particles (n)	640	74	296	44	2
Membrane (μm)	432.6	308.9	308.8	28.8	34.7
Gold particles/μm	1.48 ± 0.10	0.24 ± 0.06	0.96 ± 0.10	1.53 ± 0.30	0.06 ± 0.06
Control					
Gold particles (n)	33	7	10	4	2
Membrane (μm)	303.1	109.8	138.1	31.7	6.2
Gold particles/μm	0.11 ± 0.02	0.06 ± 0.03	0.07 ± 0.03	0.13 ± 0.06	0.32 ± 0.18

Gold particles associated with the indicated membrane organelles were counted and the density per μm membrane length determined. Control labeling was determined using a nonimmune rat IgM antibody (Benlimame *et al.*, 1995).

Under these conditions, the extent of punctate and tubular labeling varied between cells. Fibrillar labeling of bAMF was also observed and has been determined to be localized to the cell surface (our unpublished results). An extended chase of 2 or 4 h after a 2-h pulse resulted in decreased punctate labeling and the accumulation of bAMF labeling in tubular structures that colocalized with AMF-R tubules (Figure 4, C and D). The vast majority of the cells exhibited predominantly intracellular tubular labeling as well as cell surface
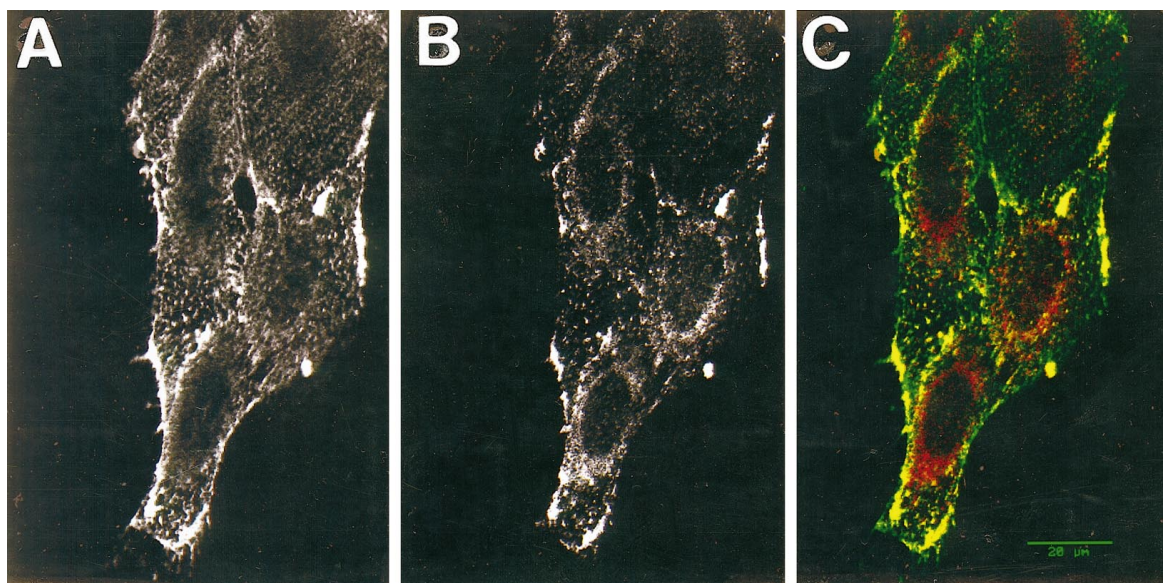

Figure 2. Colocalization of AMF-R and caveolin by confocal microscopy. Viable NIH-3T3 cells were labeled for cell surface AMF-R at 4°C (A) and for caveolin after fixation and permeabilization (B). To demonstrate the colocalization of AMF-R and caveolin, confocal images from both fluorescent channels were superimposed (panel C; AMF-R in green and caveolin in red) and colocalization appears in yellow. Bar, 20 μm.
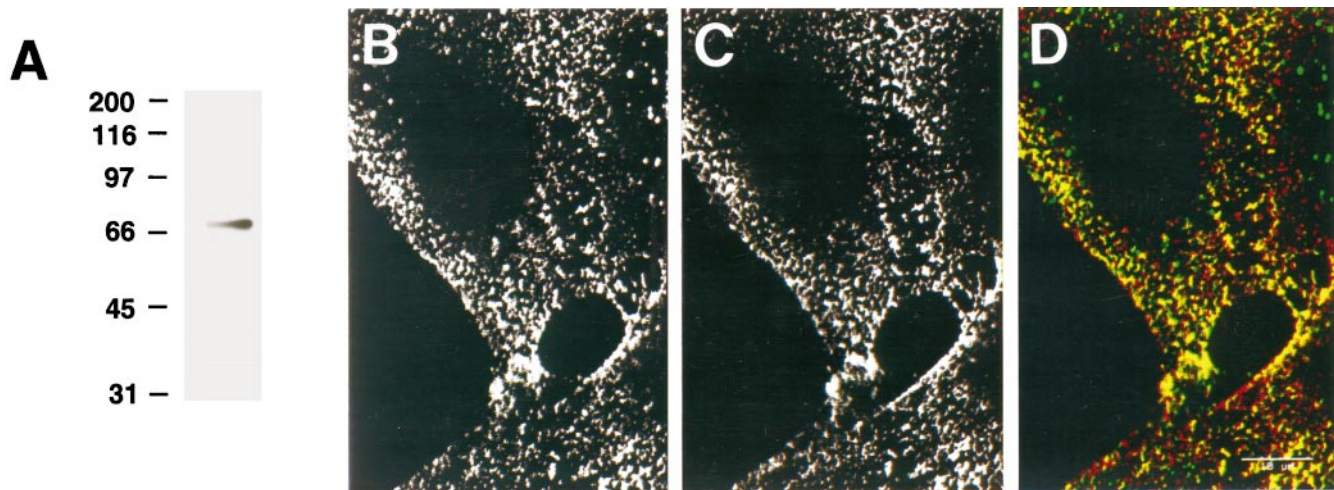
Figure 3. bAMF and anti-AMF-R mAb colocalize on the cell surface. bAMF migrated as a single band in protein blots revealed with HRP-streptavidin (A). Confocal imaging of cell surface labeling of viable NIH-3T3 cells at 4°C with bAMF (B) or anti-AMF-R antibody (C). Confocal images from both fluorescent channels were superimposed (panel D; bAMF in green and AMF-R in red) and revealed a significant degree of colocalization in yellow. Bar, 20 μm.

fibrillar labeling. After treatment of cells with acidified medium (pH 5.5) and disruption of clathrin-coated pits and vesicles (Heuser, 1989), bAMF internalized for 1 h is localized to intracellular AMF-R tubules (Figure 4, E and F). In the acidified medium, internalized transferrin did not cluster in the perinuclear recycling compartment, demonstrating that the acidification procedure did indeed disrupt clathrin-mediated endocytosis (Figure 4, G and H). bAMF is therefore internalized via a clathrin-independent endocytic pathway to the smooth ER.

The colocalization of bAMF-labeled tubules with AMF-R tubules was confirmed by confocal microscopy (Figure 5). After a 1-h bAMF internalization, internalized bAMF is localized to tubular structures that colocalize with AMF-R tubules (Figure 5, A–C) as well as to punctate structures that exhibit partial colocalization with LAMP-1–positive lysosomes (Figure 5, D–F). As seen here, the intense punctate labeling can hide the fainter tubular labeling of bAMF in some cells (Figures 4A and 5D). In acidification medium, the vast majority of bAMF labeling, aside from cell surface fibrils, is localized to tubules that colocalize with AMF-R tubules (Figure 5, G–I). bAMF internalized for 1 h in the presence of a 10-fold excess of unlabeled AMF is localized only to punctate structures, and no labeling of AMF-R tubules can be detected (Figure 5, J–L). While the extent of tubular labeling of bAMF varies between cells under control conditions (Figure 5, A and D), in the presence of excess unlabeled AMF the localization of bAMF to AMF-R tubules is never observed (Figure 5, J–L). bAMF internalization to intracellular AMF-R tubules therefore occurs via a receptor-mediated process. The inability of excess AMF

to block bAMF internalization to punctate perinuclear structures, which exhibit partial colocalization with LAMP-1–labeled lysosomes (our unpublished observations), demonstrates that this labeling is not saturable and corresponds to nonspecific fluid phase uptake. The disappearance of lysosomal labeling after extended chase times (Figure 4, C and D) is therefore most likely due to lysosomal degradation of fluid phase-internalized bAMF.

The location of bAMF internalized at 37°C was determined by postembedding electron microscopy with streptavidin–10 nm gold. After a 10-min pulse bAMF could be detected in caveolae (Figure 6, A and B). After a 30-min pulse, both caveolae and intracellular smooth and rough ER elements were labeled (Figure 6, C–G). Dense structures morphologically equivalent to lysosomes are also labeled and presumably correspond to the perinuclear structures densely labeled for internalized bAMF by immunofluorescence (Figure 6, H and I).

DISCUSSION

AMF-R Localization to Caveolae

Caveolae are smooth plasmalemmal vesicles whose cytoplasmic surface presents a spiral coat containing the 21-kDa caveolae-specific phosphoprotein caveolin

---

Figure 4 (facing page). Internalization of bAMF to AMF-R tubules. NIH-3T3 cells were pulse labeled with bAMF at 37°C for 1 h (A and B), for 2 h and chased for 4 h (C and D), or for 1 h in medium acidified to pH 5.5 to disrupt clathrin-mediated endocytosis (E and
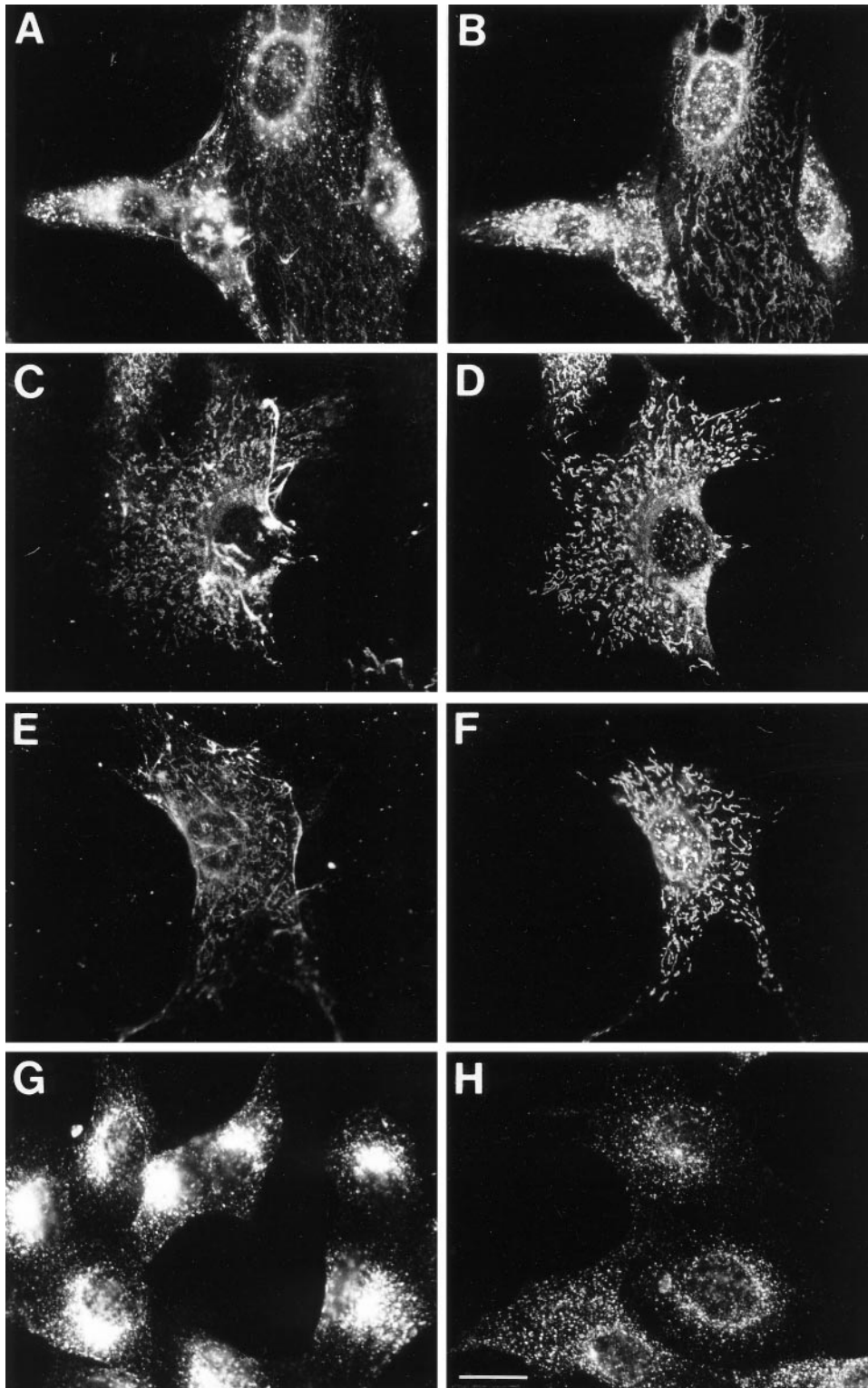
Figure 4. F). After fixation with methanol/acetone, cells were double labeled with Texas Red-streptavidin to reveal bAMF (A, C, and E) and anti-AMF-R mAb and FITC-conjugated anti-rat secondary antibody to reveal AMF-R labeling (B, D, and F). To ensure that cellular acidification disrupted clathrin-mediated endocytosis of transferrin receptor, NIH-3T3 cells were incubated at 37°C with Texas Red transferrin for 30 min in regular medium (G) or in medium acidified to pH 5.5 (H). Bar, 20 μm.
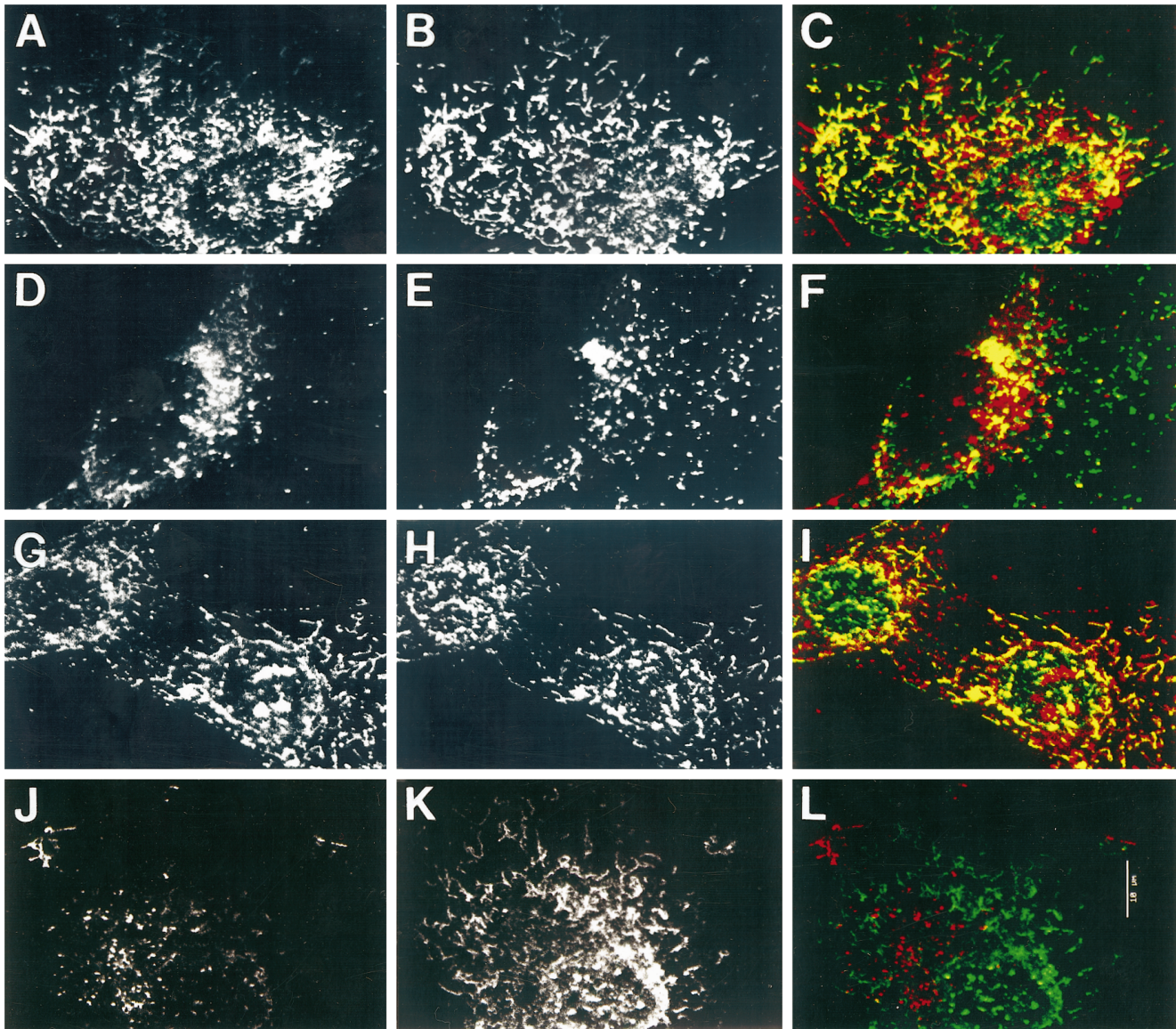
Figure 5. Localization of internalized bAMF to AMF-R tubules by confocal microscopy. NIH-3T3 cells were pulse labeled with bAMF at 37°C for 1 h in regular medium (A–F) for 1 h in medium acidified to pH 5.5 to disrupt clathrin-mediated endocytosis (G–I), or in regular medium in the presence of 10-fold excess unlabeled AMF (J–L) before fixation with methanol/acetone. bAMF was revealed with Texas Red-streptavidin (A, D, G, and J) and AMF-R (B, H, and K) or LAMP-1 (E) labeled with the appropriate primary antibodies and FITC-conjugated secondary antibodies. Confocal images from both fluorescent channels were superimposed (panels C, I, and L, bAMF in red and AMF-R in green; panel F, bAMF in red and LAMP-1 in green) and colocalization appears in yellow. Bar, 10 μm.

(Rothberg *et al.*, 1992). By postembedding immuno-electron microscopy, AMF-R is localized to morpho-logically identifiable caveolae as well as to smooth ER tubules (Figure 1 and Table 1). In contrast to polarized epithelial MDCK cells (Benlimame *et al.*, 1995), label-ing of rough ER tubules was not above background in either NIH-3T3 or HeLa cells, indicating that AMF-R is a specific marker for smooth ER in these two cell types. The localization of AMF-R to caveolae was con-firmed by the colocalization of cell surface AMF-R,

labeled by the addition of anti-AMF-R to viable cells at 4°C, with caveolin by confocal fluorescence micros-copy (Figure 2). By both postembedding immunoelec-tron microscopy and confocal double labeling with caveolin, only a minor portion of cell surface AMF-R actually is distributed to caveolae identified either morphologically or by the presence of caveolin. Whether flat plasma membrane regions to which AMF-R is localized are equivalent to cholesterol-rich Triton X-100–insoluble glycolipid rafts (Brown and
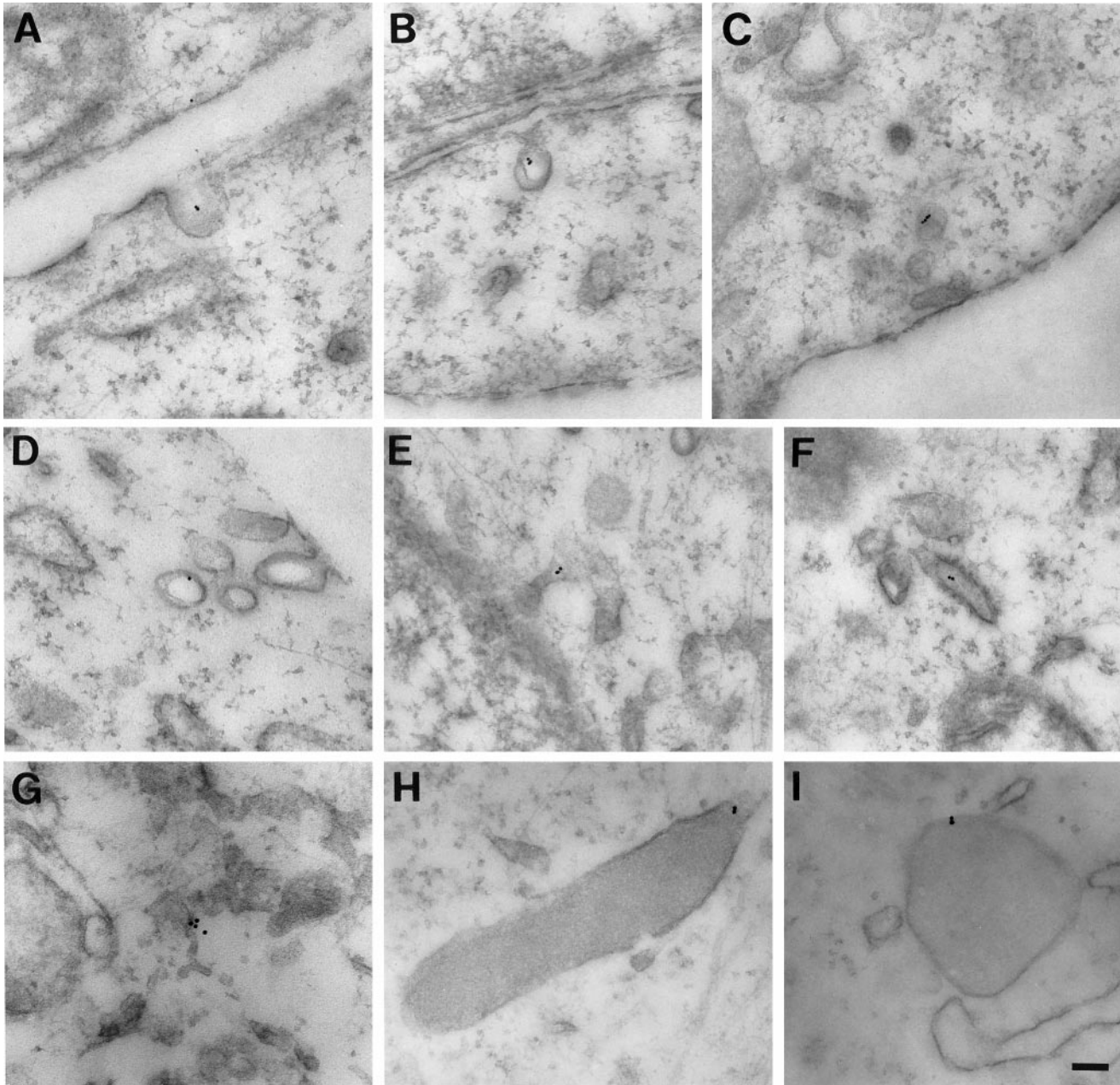
Figure 6. Electron microscopy of the internalization pathway of bAMF. NIH-3T3 cells were pulsed with bAMF at 37°C for 10 (A, B, and H) or 30 min (C, D, E, F, G, and I). The localization of bAMF was revealed by postembedding labeling with 10-nm gold-conjugated streptavidin. After 10 min, bAMF is localized to cell surface caveolae (A and B). After a 30-min pulse, bAMF is localized to caveolae and smooth vesicles (C and D) and also appears in intracellular membranous tubules (E, F, and G) including distinctive smooth (E) and rough (F) ER elements. bAMF labeling of dense lysosomal structures is also detected (H and I). Bar, 0.1 μm.

Rose, 1992; Sargiacomo *et al.*, 1993; Chang *et al.*, 1994) is difficult to assess due to the large quantity of AMF-R localized to intracellular tubules (61% in NIH-3T3 and 74% in HeLa; see Table 1). Based on the labeling of AMF-R by immunoelectron microscopy, only ~5% of total cellular AMF-R is actually localized to caveolae (Table 1).

Transduction of the AMF motility signal is mediated by a pertussis toxin-sensitive G protein, phosphorylation of AMF-R, and both PKC and tyrosine kinase activities (Stracke *et al.*, 1987; Nabi *et al.*, 1990; Watanabe *et al.*, 1991; Timar *et al.*, 1993; Kanbe *et al.*, 1994). Heterotrimeric G proteins, including the pertussis toxin-sensitive $G_{\alpha i2}$ protein, have been shown to associate

with caveolar domains (Sargiacomo *et al.*, 1993; Chang *et al.*, 1994; Schnitzer *et al.*, 1995) although results from another study indicate that heterotrimeric G proteins do not associate with an immunoisolated caveolae fraction (Stan *et al.*, 1997). The AMF-R sequence codes for a putative type 1 membrane protein and contains within its cytoplasmic domain a consensus sequence for a G protein activator motif (Watanabe *et al.*, 1991; Okamoto and Nishimoto, 1992; Silletti *et al.*, 1996). The association of AMF-R with caveolae could serve to facilitate its interaction with heterotrimeric G proteins after receptor activation. Caveolin was originally identified as a phosphorylated substrate of Rous sarcoma virus tyrosine kinase, and tyrosine kinase activities have been localized to caveolae (Glenney, 1989; Sargiacomo *et al.*, 1993; Shenoy-Scaria *et al.*, 1994; Robbins *et al.*, 1995; Liu *et al.*, 1997). The flattening of caveolae at the plasma membrane is stimulated by the PKC stimulator, phorbol 12-myristate 13-acetate, and the okadaic acid-mediated internalization of caveolae is blocked by the kinase inhibitor staurosporine, suggesting that PKC activity may be associated with caveolae (Smart *et al.*, 1993; Parton *et al.*, 1994). The involvement of heterotrimeric G proteins as well as tyrosine kinase and PKC activities in transduction of the AMF motility signal is consistent with the localization of AMF-R to cell surface caveolae.

Clathrin-independent Internalization of AMF-R to Smooth ER Tubules

The presence of AMF-R both at the cell surface and within an intracellular ER-associated organelle suggested that the receptor recycles between these two cellular sites (Nabi *et al.*, 1992; Benlimame *et al.*, 1995). Caveolae have been implicated in transcytosis in endothelial cells (Palade *et al.*, 1979; Ghitescu *et al.*, 1986; Schnitzer *et al.*, 1994), and interaction between caveolae and smooth ER has been proposed for the vascular endothelium (Bundgaard, 1991). The inositol triphosphate receptor-like protein has been localized to caveolae, and this protein is expressed not only at the plasma membrane but also within the ER (Fujimoto *et al.*, 1992; Sharp *et al.*, 1992). The fact that the density of AMF-R labeling within caveolae is equivalent to (NIH-3T3) or greater than (HeLa) that of smooth vesicles and tubules is consistent with the concentration of AMF-R within caveolae before vesicle budding and fusion with AMF-R tubules (Table 1).

AMF exhibits sequence identity to phosphohexose isomerase (Watanabe *et al.*, 1996). Biotinylated phosphohexose isomerase or bAMF colocalizes with cell surface AMF-R labeled with antibodies to AMF-R at 4°C and is endocytosed by cells at 37°C to tubules that colocalize with smooth ER AMF-R tubules by confocal microscopy and to morphologically identifiable ER tubules by electron microscopy. bAMF internalization to smooth ER tubules is a receptor-mediated process as it can be blocked by the presence of excess unlabeled AMF. Cellular acidification, which specifically blocks clathrin-mediated endocytosis, disrupts the internalization of transferrin, but not that of bAMF to AMF-R tubules, demonstrating that AMF-R is internalized to AMF-R tubules via a nonclathrin endocytic pathway. Under the conditions used in these experiments, internalization of bAMF to lysosomal structures is also observed. This lysosomal labeling is observed even in the presence of excess unlabeled AMF, indicating that it is not receptor-mediated and due to fluid phase uptake. We have therefore identified a clathrin-independent AMF-R–mediated endocytic pathway that targets bAMF to the ER. The localization of AMF-R and internalized bAMF to cell surface caveolae by electron microscopy implicates these smooth invaginations of the plasma membrane in the endocytosis of AMF-R to the smooth ER subdomain for which it is a marker (Benlimame *et al.*, 1995; Wang *et al.*, 1997).

Role of Caveolae in AMF-R Internalization

Whether caveolae are involved in endocytic processes in nonendothelial cells remains a controversial subject. The transient opening and shutting of caveolae at the cell surface, in the absence of dissociation from the plasma membrane, creates localized ligand concentrations, which enter the cell via a process called potocytosis (Anderson *et al.*, 1992). Caveolin-positive intracellular endocytic structures have been identified in elicited macrophages (Kiss and Geuze, 1997). Clathrin-independent internalization of the cholecystokinin receptor, apparently via caveolae, targeted the receptor only to subplasmalemmal vesicles (Roettger *et al.*, 1995). Non-clathrin–mediated endocytosis has been identified in nonendothelial cells for a number of ligands, among them cholera toxin, ricin, and the β-adrenergic receptor (Montesano *et al.*, 1982; Sandvig *et al.*, 1987; Raposo *et al.*, 1989). Cholera toxin and ricin are targeted to the same endosomes as transferrin receptor (Tran *et al.*, 1987; Hansen *et al.*, 1993), indicating that ligands internalized via clathrin and nonclathrin invaginations can follow the endosomal/lysosomal pathway. Disruption of clathrin polymerization does not influence the extent of bulk flow internalization (Cupers *et al.*, 1994) and whether these clathrin-independent internalization routes involve caveolae or clathrin-coated pits without the clathrin remains to be determined (van Deurs *et al.*, 1993).

The receptor-mediated endocytosis of bAMF not to endosomes and lysosomes but to the ER certainly suggests that bAMF endocytosis is not mediated by uncoated clathrin vesicles. Internalization of anti-AMF-R mAb to intracellular tubular structures has also been visualized in metastatic K1735 melanoma

cell variants (Silletti *et al.*, 1994). Furthermore, alternate internalization routes involving caveolae have been described. Treatment of A431 cells with the phosphatase inhibitor okadaic acid enhances the ability of caveolae labeled with cholera toxin to dissociate from the plasma membrane; internalized cholera toxin was targeted to intracellular tubular profiles and clusters of caveolae, some of which were not labeled by fluid phase uptake (Parton *et al.*, 1994). Cholesterol depletion results in the internalization of caveolin and its recycling via the ER, ERGIC, and the Golgi apparatus to the plasma membrane (Smart *et al.*, 1994; Conrad *et al.*, 1995). SV40 virus associates with caveolae and is internalized via smooth plasmalemmal vesicles to smooth tubules that are extensions of the ER (Kartenbeck *et al.*, 1989; Anderson *et al.*, 1996; Stang *et al.*, 1997). The internalization pathway of SV40 to the ER (Kartenbeck *et al.*, 1989) is therefore remarkably similar to that of AMF-R described here, and the localization of both AMF-R and SV40 to cell surface caveolae certainly implicates caveolae in this ER-directed endocytic pathway. It can be argued that the caveolae to which AMF-R is localized at steady state are not necessarily involved in its clathrin-independent endocytosis; however, we would argue that the best interpretation of our data is that AMF-R internalization to the ER occurs via caveolae. Distinct receptor-mediated caveolae internalization pathways have been described in endothelial cells of the rete mirabile (Bendayan and Rasio, 1996), and it is conceivable that morphologically indistinguishable but functionally distinct subpopulations of caveolae exist. AMF activation of AMF-R may stimulate both transduction of the AMF motility-stimulating signal and internalization of AMF-R, perhaps within the same cell surface caveolar domain.

The identification of caveolin as a phosphorylated substrate for the src tyrosine kinase is indicative of a role for caveolae in cellular transformation (Glenney, 1989). AMF-R localization to these cell surface structures further implicates them in tumor cell malignancy and metastasis. Oncogene transformation of NIH-3T3 cells results in the loss of caveolin expression and disappearance of caveolae (Koleske *et al.*, 1995) while treatment with the tumor promotor, phorbol 12-myristate 13-acetate, also results in the disappearance of caveolar invaginations (Smart *et al.*, 1993). In lymphocytes or Sf21 insect cells that lack caveolin and caveolae, the formation of cell surface caveolae as well as intracellular caveolar vesicles can be induced after transfection with caveolin, suggesting that caveolin expression is necessary for caveolar invagination (Fra *et al.*, 1995; Li *et al.*, 1996). Alternatively, caveolin may serve to stabilize caveolar invaginations at the cell surface.

AMF Recycling and Cell Motility

The established role of AMF-R in cell motility and metastasis implicates AMF-R internalization, and subsequent recycling to the cell surface, in the motile process (Nabi *et al.*, 1992; Silletti and Raz, 1996). The potential involvement of a caveolae-mediated recycling pathway via an ER-associated organelle in cell motility complements the previously described role for coated pit internalization and recycling (Bretscher, 1984; Altankov and Grinnell, 1993), the targeting of Golgi-derived membrane vesicles (Bergmann *et al.*, 1983; Rogalski *et al.*, 1984; Peränen *et al.*, 1996), and the recycling of early endosomal or lysosomal proteins (Bretscher, 1989; Garrigues *et al.*, 1994; Hopkins *et al.*, 1994) in cellular movement. The extension of lamellipodia by the motile cell requires the continual generation of de novo polarized membrane domains. The targeting of the bulk of intracellular membrane traffic toward the site of formation of new membrane domains, the leading edge, is therefore not surprising. Targeting of intracellular membrane traffic is, in large part, mediated by the microtubule cytoskeleton (Kelly, 1990; Cole and Lippincott-Schwartz, 1995) whose role in determining the directionality of membrane traffic to the leading edge as well as the directionality of cell movement has been demonstrated (Rogalski *et al.*, 1984; Tanaka *et al.*, 1995). AMF-R tubules associate with a pericentriolar microtubule subdomain enriched in stabilized microtubules in Moloney sarcoma virus-transformed epithelial MDCK cells, supporting a role for microtubules in the intracellular targeting of AMF-R tubules (Nabi *et al.*, 1997). The role of microtubules in the directionality of lamellipodial extension and cell movement may be to target intracellular membrane traffic to the leading edge of the motile cell. It should be noted, however, that while cells in serum culture are continually motile, cell motility in situ occurs in response to specific motile stimuli (Stoker and Gherardi, 1991). A recycling pathway stimulated by a cytokine, such as AMF, may represent a motility-specific membrane-targeting pathway.

ACKNOWLEDGMENTS

REFERENCES

Altankov, G., and Grinnell, F. (1993). Depletion of intracellular potassium disrupts coated pits and reversibly inhibits cell polarization during fibroblast spreading. J. Cell Biol. *120*, 1449–1459.

Anderson, H.A., Chen, Y., and Norkin, L.C. (1996). Bound simian virus 40 translocates to caveolin-enriched membrane domains, and its entry is inhibited by drugs that selectively disrupt caveolae. Mol. Biol. Cell 7, 1825–1834.

Anderson, R.G.W., Kamen, B.A., Rothberg, K.G., and Lacey, S.W. (1992). Potocytosis: sequestration and transport of small molecules by caveolae. Science 253, 410–411.

Bendayan, M., and Rasio, E.A. (1996). Transport of insulin and albumin by the microvascular endothelium of the rete mirabile. J. Cell Sci. 109, 1857–1864.

Benlimame, N., Simard, D., and Nabi, I.R. (1995). Autocrine motility factor receptor is a marker for a distinct tubular membrane organelle. J. Cell Biol. 129, 459–471.

Bergmann, J.E., Kupfer, A., and Singer, S.J. (1983). Membrane insertion at the leading edge of motile fibroblasts. Proc. Natl. Acad. Sci. USA 80, 1367–1371.

Bretscher, M.S. (1984). Endocytosis: relation to capping and cell locomotion. Science 226, 681–686.

Bretscher, M.S. (1989). Endocytosis and recycling of the fibronectin receptor in CHO cells. EMBO J. 8, 1341–1348.

Bretscher, M.S. (1996). Getting membrane flow and the cytoskeleton to cooperate in moving cells. Cell 87, 601–606.

Brown, D.A., and Rose, J.K. (1992). Sorting of GPI-anchored proteins in glycolipid enriched membrane subdomains during transport to the apical cell surface. Cell 68, 533–544.

Bundgaard, M. (1991). The three-dimensional organization of smooth endoplasmic reticulum in capillary endothelia: its possible role in regulation of free cytosolic calcium. J. Struct. Biol. 107, 76–85.

Chang, W.-J., Ying, Y.-s., Rothberg, K.G., Hooper, N.M., Turner, A.J., Gambliel, H.A., De Gunzberg, J., Mumby, S.M., Gilman, A.G., and Anderson, R.G.W. (1994). Purification and characterization of smooth muscle caveolae. J. Cell Biol. 126, 127–138.

Cole, N.B., and Lippincott-Schwartz, J. (1995). Organization of organelles and membrane traffic by microtubules. Curr. Opin. Cell Biol. 7, 55–64.

Condeelis, J. (1993). Life at the leading edge: the formation of cell protrusions. Annu. Rev. Cell Biol. 9, 411–444.

Conrad, P.A., Smart, E.J., Ying, Y.-S., Anderson, R.G.W., and Bloom, G.S. (1995). Caveolin cycles between plasma membrane caveolae and the Golgi complex by microtubule-dependent and microtubule-independent steps. J. Cell Biol. 131, 1421–1433.

Cupers, P., Veithen, A., Kiss, A., Baudhuin, P., and Courtoy, P.J. (1994). Clathrin polymerization is not required for bulk-phase endocytosis in rat fetal fibroblasts. J. Cell Biol. 127, 725–735.

Dotti, C.G., and Simons, K. (1990). Polarized sorting of viral glycoproteins to the axons and dendrites of hippocampal neurons in culture. Cell 62, 63–72.

Drubin, D.G., and Nelson, W.J. (1996). Origins of cell polarity. Cell 84, 335–344.

Fra, A.M., Williamson, E., Simons, K., and Parton, R.G. (1995). De novo formation of caveolae in lymphocytes by expression of VIP21-caveolin. Proc. Natl. Acad. Sci. USA 92, 8655–8659.

Fujimoto, T., Nakade, S., Miyawaki, A., Mikoshiba, K., and Ogawa, K. (1992). Localization of 1,4,5-triphosphate receptor-like protein in plasmalemmal caveolae. J. Cell Biol. 119, 1507–1513.

Garrigues, J., Anderson, J., Hellström, K.E., and Hellström, I. (1994). Anti-tumor antibody BR96 blocks cell migration and binds to a lysosomal membrane glycoprotein on cell surface microspikes and ruffled membranes. J. Cell Biol. 125, 129–142.

Ghitescu, L., Fixman, A., Simionescu, M., and Simionescu, N. (1986). Specific binding sites for albumin restricted to plasmalemmal vesicles of continuous capillary endothelium: receptor-mediated transcytosis. J. Cell Biol. 102, 1304–1311.

Glenney, J.R. (1989). Tyrosine phosphorylation of a 22-kDa protein is correlated with transformation by Rous Sarcoma virus. J. Biol. Chem. 264, 20163–20166.

Guirguis, R., Javadpour, N., Sharareh, S., Biswas, C., el-Amin, W., Mansur, I., and Kim, J.S. (1990). A new method for evaluation of urinary autocrine motility factor and tumor cell collagenase stimulating factor as markers for urinary tract cancers. J. Occup. Med. 32, 846–853.

Hansen, S.H., Sandvig, K., and van Deurs, B. (1993). Molecules internalized by clathrin-independent endocytosis are delivered to endosomes containing transferrin receptors. J. Cell Biol. 123, 89–97.

Heuser, J. (1989). Effects of cytoplasmic acidification on clathrin lattice morphology. J. Cell Biol. 108, 401–411.

Hirono, Y., Fushida, S., Yonemura, Y., Yamamoto, H., Watanabe, H., and Raz, A. (1996). Expression of autocrine motility factor receptor correlates with disease progression in human gastric cancer. Br. J. Cancer 74, 2003–2007.

Hopkins, C.R., Gibson, A., Shipman, M., Strickland, D.K., and Trowbridge, I.S. (1994). In migrating fibroblasts, recycling receptors are concentrated in narrow tubules in the pericentriolar area, and then routed to the plasma membrane of the leading lamella. J. Cell Biol. 125, 1265–1274.

Kanbe, K., Chigara, M., and Watanabe, H. (1994). Effects of protein kinase inhibitors on the cell motility stimulated by autocrine motility factor. Biochim. Biophys. Acta 1222, 395–399.

Kartenbeck, J., Stukenbrok, H., and Helenius, A. (1989). Endocytosis of simian virus 40 into the endoplasmic reticulum. J. Cell Biol. 109, 2721–2729.

Keller, P., and Simons, K. (1997). Post-Golgi biosynthetic trafficking. J. Cell Sci. 110, 3001–3009.

Kelly, R.B. (1990). Microtubules, membrane traffic, and cell organization. Cell 61, 5–7.

Kiss, A.L., and Geuze, H.J. (1997). Caveolae can be alternative endocytic structures in elicited macrophages. Eur. J. Cell Biol. 73, 19–27.

Koleske, A.J., Baltimore, D., and Lisanti, M.P. (1995). Reduction of caveolin and caveolae in oncogenically transformed cells. Proc. Natl. Acad. Sci. USA 92, 1381–1385.

Li, S., Song, K.S., Koh, S.S., Kikuchi, A., and Lisanti, M.P. (1996). Baculovirus-based expression of mammalian caveolin in Sf21 insect cells. J. Biol. Chem. 271, 28647–28654.

Liotta, L.A., Mandler, R., Murano, G., Katz, D.A., Gordon, R.K., Chiang, P.K., and Schiffman, E. (1986). Tumor cell autocrine motility factor. Proc. Natl. Acad. Sci. USA 83, 3302–3306.

Liu, P., Ying, Y.-s., and Anderson, R.G.W. (1997). Platelet-derived growth factor activated mitogen-activated protein kinase in isolated caveolae. Proc. Natl. Acad. Sci. USA 94, 13666–13670.

Montesano, R., Roth, J., Robert, A., and Orci, L. (1982). Non-coated membrane invaginations are involved in binding and internalization of cholera and tetanus toxins. Nature 296, 651–653.

Nabi, I.R., Guay, G., and Simard, D. (1997). AMF-R tubules concentrate in a pericentriolar microtubule domain following transformation of MDCK epithelial cells. J. Histochem. Cytochem. 45, 1351–1363.

Nabi, I.R., Watanabe, H., and Raz, A. (1990). Identification of B16–F1 melanoma autocrine motility-like factor receptor. Cancer Res. 50, 409–414.

Nabi, I.R., Watanabe, H., and Raz, A. (1992). Autocrine motility factor and its receptor: role in cell locomotion and metastasis. Cancer Metastasis Rev. *11*, 5–20.

Nakamori, S., Watanabe, H., Kameyama, M., Imaoka, S., Furukawa, H., Ishikawa, O., Sasaki, Y., Kabuto, T., and Raz, A. (1994). Expression of autocrine motility factor receptor in colorectal cancer as a predictor for disease recurrence. Cancer *74*, 1855–1862.

Okamoto, T., and Nishimoto, I. (1992). Detection of G protein-activator regions in M_4 subtype muscarinic, cholinergic, and α_2-adrenergic receptors based upon characteristics in primary structure. J. Biol. Chem. *267*, 8342–8346.

Otto, T., Birchmeier, W., Schmidt, U., Hinke, A., Schipper, J., Rübben, H., and Raz, A. (1994). Inverse relation of E-cadherin and autocrine motility factor receptor expression as a prognostic factor in patients with bladder carcinomas. Cancer Res. *54*, 3120–3123.

Palade, G., Simionescu, M., and Simionescu, N. (1979). Structural aspects of the permeability of the microvascular endothelium. Acta Physiol. Scand. *463*, 11–32.

Parton, R.G., Joggerst, B., and Simons, K. (1994). Regulated internalization of caveolae. J. Cell Biol. *127*, 1199–1215.

Peränen, J., Auvinen, P., Virta, H., Wepf, R., and Simons, K. (1996). Rab8 promotes polarized membrane transport through reorganization of actin and microtubules in fibroblasts. J. Cell Biol. *135*, 153–167.

Raposo, G., Dunia, I., Delavier-Klutchko, C., Kaveri, S., Strosberg, A.D., and Benedetti, E.L. (1989). Internalization of beta-adrenergic receptor in A431 cells involves non-coated vesicles. Eur. J. Cell Biol. *50*, 340–352.

Rinnerthaler, G., Geiger, B., and Small, J.V. (1988). Contact formation during fibroblast locomotion: involvement of membrane ruffles and microtubules. J. Cell Biol. *106*, 747–760.

Robbins, S.M., Quintrell, N.A., and Bishop, J.M. (1995). Myristolation and differential palmitoylation of the HCK protein-tyrosine kinases govern their attachment to membranes and association with caveolae. Mol. Cell Biol. *15*, 3507–3515.

Rodriguez-Boulan, E., and Powell, S.K. (1992). Polarity of epithelial and neuronal cells. Annu. Rev. Cell Biol. *8*, 395–427.

Rodriguez-Boulan, E., and Sabatini, D. (1978). Asymmetric budding of viruses in epithelial monolayers: a model system for the study of epithelial polarity. Proc. Natl. Acad. Sci. USA *75*, 5071–5075.

Roettger, B.F., Rentsch, R.U., Pinon, D., Holicky, E., Hadac, E., Larkin, J.M., and Miller, L.J. (1995). Dual pathways of internalization of the cholecystokinin receptor. J. Cell Biol. *128*, 1029–1041.

Rogalski, A.A., Bergmann, J.E., and Singer, S.J. (1984). Effect of microtubule assembly status on the intracellular processing and surface expression of an integral protein of the plasma membrane. J. Cell Biol. *99*, 1101–1109.

Rothberg, K.G., Heuser, J.E., Donzell, W.C., Ying, Y.-S., Glenney, J.R., and Anderson, R.G.W. (1992). Caveolin, a protein component of caveolae membrane coats. Cell *68*, 673–682.

Sandvig, K., Olsnes, S., Petersen, O.W., and van Deurs, B. (1987). Acidification of the cytosol inhibits endocytosis from coated pits. J. Cell Biol. *105*, 679–689.

Sargiacomo, M., Sudol, M., Tang, Z., and Lisanti, M.P. (1993). Signal transducing molecules and GPI-linked proteins form a caveolin-rich insoluble complex in MDCK cells. J. Cell Biol. *122*, 789–808.

Schnitzer, J.E., Liu, J., and Oh, P. (1995). Endothelial caveolae have the molecular transport machinery for vesicle budding, docking, and fusion including the VAMP, NSF, SNAP, annexins, and GTPases. J. Biol. Chem. *270*, 14399–14404.

Schnitzer, J.E., Oh, P., Pinney, E., and Allard, J. (1994). Filipin-sensitive caveolae-mediated transport in endothelium: reduced transcytosis, scavenger endocytosis, and capillary permeability of select macromolecules. Proc. Natl. Acad. Sci. USA *127*, 1217–1232.

Sharp, A.H., Snyder, S.H., and Nigam, S.K. (1992). Inositol 1,4,5-triphosphate receptors. Localization in epithelial tissue. J. Biol. Chem. *267*, 7444–7449.

Shenoy-Scaria, A.M., Dietzen, D.J., Kwong, J., Link, D.C., and Lublin, D.M. (1994). Cysteine[3] of Src family protein tyrosine kinases determines palmitoylation and localization in caveolae. J. Cell Biol. *126*, 353–363.

Silletti, S., Paku, S., and Raz, A. (1996). Tumor autocrine motility factor responses are mediated through cell contact and focal adhesion rearrangement in the absence of new tyrosine phosphorylation in metastatic cells. Am. J. Pathol. *148*, 1649–1660.

Silletti, S., and Raz, A. (1993). Autocrine motility factor is a growth factor. Biochem. Biophys. Res. Commun. *194*, 446–457.

Silletti, S., and Raz, A. (1996). Regulation of autocrine motility factor receptor expression in tumor cell locomotion and metastasis. Curr. Topics Microbiol. Immunol. *213/II*, 137–169.

Silletti, S., Timar, J., Honn, K.V., and Raz, A. (1994). Autocrine motility factor induces differential 12-lipoxygenase expression and activity in high and low-metastatic K1735 melanoma cell variants. Cancer Res. *54*, 5752–5756.

Simard, D., and Nabi, I.R. (1996). Inverse relation of autocrine motility factor receptor and E-cadherin expression following transformation of epithelial MDCK cells. Biochem. Biophys. Res. Commun. *219*, 122–127.

Singer, S.J., and Kupfer, A. (1986). The directed migration of eukaryotic cells. Annu. Rev. Cell Biol. *2*, 337–365.

Smart, E.J., Foster, D., Ying, Y.-S., Kamen, B.A., and Anderson, R.G.W. (1993). Protein kinase C activators inhibit receptor-mediated potocytosis by preventing internalization of caveolae. J. Cell Biol. *124*, 307–313.

Smart, E.J., Ying, Y.-S., Conrad, P.A., and Anderson, R.G.W. (1994). Caveolin moves from caveolae to the Golgi apparatus in response to cholesterol oxidation. J. Cell Biol. *127*, 1185–1197.

Stan, R.-V., Roberts, W.G., Predescu, D., Ihida, K., Saucan, L., Ghitescu, L., and Palade, G.E. (1997). Immunoisolation and partial characterization of endothelial plasmalemmal vesicles (caveolae). Mol. Biol. Cell *8*, 595–605.

Stang, E., Kartenbeck, J., and Parton, R.G. (1997). Major histocompatibility complex class I molecules mediate association of SV40 with caveolae. Mol. Biol. Cell *8*, 47–57.

Stoker, M., and Gherardi, E. (1991). Regulation of cell movement: the motogenic cytokines. Biochim. Biophys. Acta *1072*, 81–102.

Stossel, T.P. (1993). On the crawling of animal cells. Science *260*, 1086–1094.

Stracke, M.L., Guirguis, R., Liotta, L.A., and Schiffman, E. (1987). Pertussis toxin inhibits stimulated motility independently of the adenylate cyclase pathway in human melanoma cells. Biochem. Biophys. Res. Commun. *146*, 339–345.

Takizawa, P.A., Yucei, J.K., Veit, B., Faulkner, D.J., Deerinck, T., Soto, G., Ellisman, M., and Malhotra, V. (1993). Complete vesiculation of Golgi membranes and inhibition of protein transport by a novel sea sponge metabolite, ilimaquinone. Cell *73*, 1079–1090.

Tanaka, E., Ho, T., and Kirschner, M.W. (1995). The role of microtubule dynamics in growth cone motility and axonal growth. J. Cell Biol. *128*, 139–155.

Timar, J., Silletti, S., Bazaz, R., Raz, A., and Honn, K.V. (1993). Regulation of melanoma cell motility by the lipoxygenase metabolite 12(S)-HETE[1]. Int. J. Cancer *55*, 1003–1010.

Tran, D., Carpentier, J.L., Sawano, F., Gorden, P., and Orci, L. (1987). Ligands internalized through coated or noncoated invaginations follow a common intracellular pathway. Proc. Natl. Acad. Sci. USA *84*, 7957–7961.

van Deurs, B., Kaae Holm, P., Sandvig, K., and Hansen, S.H. (1993). Are caveolae involved in clathrin-independent endocytosis? Trends Cell Biol. *3*, 249–251.

Wang, H.-J., Benlimame, N., and Nabi, I.R. (1997). The AMF-R tubule is a smooth ilimaquinone-sensitive subdomain of the endoplasmic reticulum. J. Cell Sci. *110*, 3043–3053.

Watanabe, H., Carmi, P., Hogan, V., Raz, T., Silletti, S., Nabi, I.R., and Raz, A. (1991). Purification of human tumor cell autocrine motility factor and molecular cloning of its receptor. J. Biol. Chem. *266*, 13442–13448.

Watanabe, H., Takehana, K., Date, M., Shinozaki, T., and Raz, A. (1996). Tumor cell autocrine motility factor is the neuroleukin/phosphohexose isomerase polypeptide. Cancer Res. *56*, 2960–2963.

Yoshimoro, T., Keller, P., Roth, M.G., and Simons, K. (1996). Different biosynthetic transport routes to the plasma membrane in BHK and CHO cells. J. Cell Biol. *133*, 247–256.